

Numerical Investigation of Skin and Subcutaneous Tissue Thermal Injury during Elevated Heating

George Oguntala^{1*}, Gbeminiyi Sobamowo², Yim-Fun Hu³

¹Biomedical Engineering, Department of Life Science, School of Health Sciences, Birmingham City University, UK

²Department of Mechanical Engineering, Faculty of Engineering, University of Lagos, Akoka, Nigeria

³Department of Biomedical and Electronic Engineering, Faculty of Engineering and Informatics, University of Bradford, UK

Abstract

The paper presents the non-Fourier bioheat transfer prediction methodology of human skin to determine skin burn injury with non-ideal properties of tissue, metabolism and blood perfusion. The dual-phase lag bioheat transfer model with the inclusion of evaporation is developed for the triple-layer skin tissues. The developed models are solved numerically using Galerkin's finite element method. Parametric studies on the effects of skin tissue properties, initial temperature, blood perfusion rate and heat transfer parameters for the thermal response and exposure time of the layers of the skin tissue are carried out. The results of the investigation are compared with experimental results in the literature. The study demonstrates that the initial tissue temperature, the thermal conductivity of the epidermis and dermis, relaxation and thermalisation time and convective heat transfer coefficient are critical parameters to examine skin burn injury threshold. The study also shows that thermal conductivity and the blood perfusion rate exhibits negligible effects on the burn injury threshold. The objective of the present study is to support the accurate quantification and assessment of skin burn injury for reliable experimentation, design and optimisation of thermal therapy delivery.

Keywords: Burns, Dual-Phase Lag Model, Finite Element Analysis, Numerical method, Thermal modelling

Nomenclature

C	Specific heat of tissue, J/KgK	T_0	Initial tissue temperature, ($^{\circ}C$)
c_b	Specific heat of blood, J/KgK	T_b	Blood temperature, ($^{\circ}C$)
V	Speed of thermal wave, m/s	ω_b	Rate of blood perfusion, s^{-1}
E_a	Denaturation activation energy, $Jmol^{-1}$	x, z	Coordinate variables, m
k	Tissue thermal conductivity W/mK	λ	Latent heat of vaporisation for water, J/Kg
l	Bromwich contour integration line		
L	Tissue slab length, m		
P	Frequency factor, s^{-1}		
q	Heat flux density, W/m^2		
Q_m	Metabolic heat generation, W/m^3		
R	Universal gas constant, $Jmol^{-1}K^{-1}$		
t	Time variable, s		
T	Tissue temperature, ($^{\circ}C$)		

Greek Symbols

Ω	Thermal damage parameter
τ_T	Delay time for phase lag of microstructural interaction, s
τ_q	Delay time for phase lag of the heating flux, s
ρ_w	Tissue water density, Kg/m^3

1. Introduction

The study on skin burns is **relevant** and timely as skin burns from thermal (direct contact with heated solid material and radiant heating), hot liquid (scald burns) and chemical mechanisms (direct contact with flames) remain a common form of thermal injury that occurs globally. Skin burns occur ubiquitously under different domains including homes, industry, and extreme situations such as in military combat. Burn victims often require long periods of rehabilitation and could receive multiple skin grafts and painful physical treatment, **which** often results in lifelong psychological and physical scars [1].

Heat transport analysis in living biological structures is critical in several diagnostic and therapeutic applications that involve temperature changes. Heat transport in human tissue is associated with different complex processes including conductive heat transfer in solid tissues, metabolic heat generation, convective heat transfer of blood circulation and external heat interaction with the ambient environment. The intense interest in thermal properties of skin to understand different thermal conditions including contact heating, laser heating, microwave radiation

* Corresponding author

Email address: George.Oguntala@bcu.ac.uk

which might lead to skin damage is unprecedented. To the best knowledge of the authors, the classical studies on heat transport of skin were based on the Pennes bioheat model [2]. The Pennes bioheat model is based on the classical Fourier's law with the assumption that the propagation speed of thermal disturbance is infinite which in physical reality is impractical. Energy propagation takes place at a finite speed as thermodynamic processes in living tissues maintain steady state condition after a certain time lag period [3]. Moreover, living tissues are highly non-homogeneous and non-uniformity and require relaxation time to accumulate enough energy to transfer to the nearest medium. Consequently, the limitations of the Pennes bioheat model are concurrently addressed by Cattaneo [4] and Vernotte [5] using the non-Fourier model to consider the finite propagation speed of heat. The resulting thermal wave model of the bioheat equation due to the wave-like behaviour of heat transport in biological structures is often regarded as the Cattaneo and Vernotte constitutive model. The bioheat thermal wave model gained its popularity due to its established experimental validations and ability to generate **more accurate** predictions than the classical Fourier law model. Several studies on bioheat transfer in skin tissue employed the thermal wave bioheat model to produce accurate predictions than the classical Fourier law model [6-11]. However, the hyperbolic or thermal wave model is restricted to micro-scale response in time and not the micro-scale response in space [11-13]. To overcome the limitations of the hyperbolic bioheat model, Tzou proposed a new model that considers the micro-scale response in space using phase lag in heat flux and temperature gradient [11]. The phase lag model is effective in freezing and thawing processes where phase change is critical for the analysis of the survival rate of biological structures [14, 15]. However, to examine the effects of microstructural interactions in the fast transient process of heat transport without phase change, the dual-phase lag (DPL) bioheat model has been employed in the literature to analyse the thermal behaviour of skin tissue under various skin conditions [16-18]. The DPL model characterises microstructural interactions in heat transport and is developed with the first-order Taylor series expansion. Different methodologies have been employed to analyse the DPL bioheat model for single, double, and triple layer thermal models [19-27]. These methods examined the difference in the physiological and thermal properties of the skin. Additionally, since phase change occurs in biological tissues over a wide range, the boundary conditions at the interface between the two adjacent layers results in highly nonlinear mathematical models. Therefore, to understand the temperature distribution within the human skin when subjected to heat, the use of numerical method is effective to reduce dependency on time-consuming and costly experimental analysis. The finite element method is efficient to simulate the temperature changes in biological tissue due to its reliable adaptability to complex geometries and complex governing equations [28-31]. Motivated from the work in [32], the present work presents the non-Fourier thermal modelling of triple-layer human skin tissue for the prediction of skin burn with non-ideal properties of tissue, metabolism and blood perfusion. To develop a more generalised predictive model, the modified DPL bioheat transfer model based on second-order Taylor expansion is employed. The modified DPL bioheat model in triple-layer skin tissue are solved numerically using Galerkin's FEM.

2. Methodology

The present study considered the effect of microstructural interactions in the transient process of heat transport to deal with the paradox of the classical Fourier's model and account for the limitations in the thermal wave model. The consideration is based on the fact that the gradient of temperature at a point in the material at time $t + \tau_T$ corresponds to the heat flux vector at the same point at time $t + \tau_q$, which can be written mathematically as:

$$q(x, t + \tau_q) = -k \nabla T(x, t + \tau_T) \quad (1)$$

where τ_q and τ_T are non-zero times and accounts for the effects of thermal inertia and microstructural interactions. τ_q is the phase-lag to establish heat flux and its associated conduction through a medium, τ_T accounts for the diffusion of induced heat by τ_q and represents the phase-lag to establish the temperature gradient across the medium when conduction occurs through the small-scale structures.

Using the second-order Taylor expansions, the DPL model can be expressed as:

$$\left(1 + \tau_q \frac{\partial}{\partial t} + \frac{\tau_q^2}{2} \frac{\partial^2}{\partial t^2}\right) \vec{q} = - \left(1 + \tau_T \frac{\partial}{\partial t} + \frac{\tau_T^2}{2} \frac{\partial^2}{\partial t^2}\right) k \nabla T \quad (2)$$

The above model covers a wide range of space and time for physical observations.

From Eq. (2), we write

$$\left(1 + \tau_q \frac{\partial}{\partial t} + \frac{\tau_q^2}{2} \frac{\partial^2}{\partial t^2}\right) \nabla \vec{q} = - \left(1 + \tau_T \frac{\partial}{\partial t} + \frac{\tau_T^2}{2} \frac{\partial^2}{\partial t^2}\right) (\nabla k \nabla T) \quad (3)$$

From the local energy balance, the equation for conservation of energy can be written as:

$$\rho c_p \frac{\partial T}{\partial t} = -\nabla \cdot \vec{q} + \omega_b c_b (T_b - T) + q_m + q_{ext} - q_{evap} \quad (4)$$

Eq. (4) can be re-arranged as:

$$-\nabla \cdot \vec{q} = \rho c_p \frac{\partial T}{\partial t} - \omega_b c_b (T_b - T) - q_m - q_{ext} + q_{evap} \quad (5)$$

by substituting Eq. (5) in Eq. (3) we arrived at

$$\begin{aligned} & \left(1 + \tau_q \frac{\tau_q^2}{\partial t} + \frac{\partial}{2} \frac{\partial^2}{\partial t^2} \right) \left(\rho c_p \frac{\partial T}{\partial t} - \omega_b c_b (T_b - T) - q_m - q_{ext} - q_{evap} \right) \\ & = \left(1 + \tau_T \frac{\tau_T^2}{\partial t} + \frac{\partial}{2} \frac{\partial^2}{\partial t^2} \right) (\nabla \cdot k \nabla T) \end{aligned} \quad (6)$$

The expansion of the above Eq. (6) gives

$$\begin{aligned} & \rho c_p \frac{\partial T}{\partial t} + \tau_q \rho c_p \frac{\partial^2 T}{\partial t^2} + \frac{\tau_q^2}{2} \rho c_p \frac{\partial^3 T}{\partial t^3} + \omega_b c_b \tau_q \frac{\partial T}{\partial t} + \omega_b c_b \frac{\tau_q^2}{2} \frac{\partial^2 T}{\partial t^2} \\ & = (\nabla \cdot k \nabla T) + \tau_T \frac{\partial}{\partial t} (\nabla \cdot k \nabla T) + \frac{\tau_T^2}{2} \frac{\partial^2}{\partial t^2} (\nabla \cdot k \nabla T) + \omega_b c_b (T_b - T) \\ & + q_m + \tau_q \frac{\partial q_m}{\partial t} + \frac{\tau_q^2}{2} \frac{\partial^2 q_m}{\partial t^2} + q_{ext} + \tau_q \frac{\partial q_{ext}}{\partial t} + \frac{\tau_q^2}{2} \frac{\partial^2 q_{ext}}{\partial t^2} - q_{evap} - \tau_q \frac{\partial q_{evap}}{\partial t} - \frac{\tau_q^2}{2} \frac{\partial^2 q_{evap}}{\partial t^2} \end{aligned} \quad (7)$$

In the above DPL model in Eq. (7), if τ_q and τ_T are set to zero, then the Pennes' model is recovered

$$\rho c_p \frac{\partial T}{\partial t} = (\nabla \cdot k \nabla T) + \omega_b c_b (T_b - T) + q_m + q_{ext} - q_{evap} \quad (8)$$

However, if τ_T is set to zero and the first-order Taylor expansion is used only in time, then the thermal wave or hyperbolic model is recovered as:

$$\begin{aligned} & \rho c_p \frac{\partial T}{\partial t} + \tau_q \rho c_p \frac{\partial^2 T}{\partial t^2} + \omega_b c_b \tau_q \frac{\partial T}{\partial t} = (\nabla \cdot k \nabla T) + \omega_b c_b (T_b - T) \\ & + q_m + \tau_q \frac{\partial q_m}{\partial t} + q_{ext} + \tau_q \frac{\partial q_{ext}}{\partial t} - q_{evap} - \tau_q \frac{\partial q_{evap}}{\partial t} \end{aligned} \quad (9)$$

Further, if τ_T is set to zero and the first-order Taylor expansion is used both in time and space, then Tzou' model in [11] is recovered as:

$$\begin{aligned} & \rho c_p \frac{\partial T}{\partial t} + \tau_q \rho c_p \frac{\partial^2 T}{\partial t^2} + \omega_b c_b \tau_q \frac{\partial T}{\partial t} = (\nabla \cdot k \nabla T) + \tau_T \frac{\partial}{\partial t} (\nabla \cdot k \nabla T) \\ & + \omega_b c_b (T_b - T) + q_m + \tau_q \frac{\partial q_m}{\partial t} + q_{ext} + \tau_q \frac{\partial q_{ext}}{\partial t} - q_{evap} - \tau_q \frac{\partial q_{evap}}{\partial t} \end{aligned} \quad (10)$$

The three-dimensional DPL model in the Cartesian coordinates gives

$$\begin{aligned} & \rho c_p \frac{\partial T}{\partial t} + \tau_q \rho c_p \frac{\partial^2 T}{\partial t^2} + \frac{\tau_q^2}{2} \rho c_p \frac{\partial^3 T}{\partial t^3} + \omega_b c_b \tau_q \frac{\partial T}{\partial t} + \omega_b c_b \frac{\tau_q^2}{2} \frac{\partial^2 T}{\partial t^2} \\ & = \frac{\partial}{\partial x} \left(k \frac{\partial T}{\partial x} \right) + \frac{\partial}{\partial y} \left(k \frac{\partial T}{\partial y} \right) + \frac{\partial}{\partial z} \left(k \frac{\partial T}{\partial z} \right) \\ & + \tau_T \frac{\partial}{\partial t} \left(\frac{\partial}{\partial x} \left(k \frac{\partial T}{\partial x} \right) \right) + \tau_T \frac{\partial}{\partial t} \left(\frac{\partial}{\partial y} \left(k \frac{\partial T}{\partial y} \right) \right) + \tau_T \frac{\partial}{\partial t} \left(\frac{\partial}{\partial z} \left(k \frac{\partial T}{\partial z} \right) \right) \\ & + \frac{\tau_T^2}{2} \frac{\partial^2}{\partial t^2} \left(\frac{\partial}{\partial x} \left(k \frac{\partial T}{\partial x} \right) \right) + \frac{\tau_T^2}{2} \frac{\partial^2}{\partial t^2} \left(\frac{\partial}{\partial y} \left(k \frac{\partial T}{\partial y} \right) \right) + \frac{\tau_T^2}{2} \frac{\partial^2}{\partial t^2} \left(\frac{\partial}{\partial z} \left(k \frac{\partial T}{\partial z} \right) \right) \\ & + \omega_b c_b (T_b - T) + q_m + \tau_q \frac{\partial q_m}{\partial t} + \frac{\tau_q^2}{2} \frac{\partial^2 q_m}{\partial t^2} + q_{ext} + \tau_q \frac{\partial q_{ext}}{\partial t} + \frac{\tau_q^2}{2} \frac{\partial^2 q_{ext}}{\partial t^2} \\ & - q_{evap} + \tau_q \frac{\partial q_{evap}}{\partial t} + \frac{\tau_q^2}{2} \frac{\partial^2 q_{evap}}{\partial t^2} \end{aligned} \quad (11)$$

2.1. Modelling Evaporation during the High Heating

Heating of skin tissue at high temperatures makes the moisture in the skin tissue, normally around 70-75% evaporates and later carbonises as illustrated in Fig. 1. At 100°C, ablation occurs and water vaporisation in the tissues leading to dehydration of the tissues. Moreover, as temperature increases (>100°C), the continuous vaporisation of the tissue results in the carbonisation of the tissues [33-35]. Without due consideration of these processes, the results from the models would differ significantly from experimental results. To this end, the vaporization terms are included in the above models to accommodate the phase change due to evaporation. Under this condition, an enthalpy-based model can be adopted [36]. In such a model, the enthalpy contains a three-part description. The first part corresponds to temperature changes in the liquid-containing tissue, the second part accounts for the latent heat of evaporation while the third part is the temperature changes in the post-phase-change tissue. Hence, without loss of generality, in the present work, a simple method is introduced to incorporate simple water-related processes into the thermal models to improve ablation models at high temperatures. Hence, the rate of heat of vaporisation is modelled as established in [37] as

$$q_{evap} = -\lambda \frac{d\rho_w}{dt} \quad (17)$$

λ and ρ_w represents the latent heat of vaporisation for water (2260kJ/Kg) and tissue water density respectively.

The tissue water density is a function of temperature and Eq. (17) using the chain rule is expressed as:

$$q_{evap} = -\lambda \frac{\partial \rho_w}{\partial T} = -\lambda \frac{\partial W}{\partial T} \cdot \frac{\partial T}{\partial t} \quad (18)$$

where $\frac{\partial W}{\partial T} < 0$ for evaporation

3. Two-dimensional DPL Model for the Triple Layer Skin Tissue

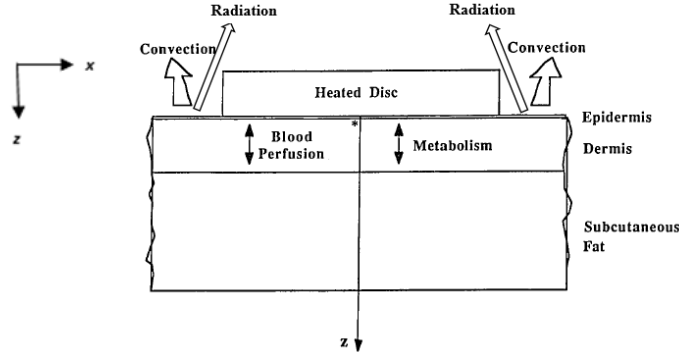


Fig. 1. Schematic diagram of the processes under consideration

In the three-layer skin tissue illustrated in Fig. 1, the two-dimensional, three-layer DPL thermal model can be written as:

$$\begin{aligned} & \rho_l \left(c_{p,l} - \frac{\lambda_l}{\rho_l} \frac{\partial W_l}{\partial T} \right) \frac{\partial T_l}{\partial t} + \tau_{q,l} \rho_l \left(c_{p,l} - \frac{\lambda_l}{\rho_l} \frac{\partial W_l}{\partial T} \right) \frac{\partial^2 T_l}{\partial t^2} + \frac{\tau_{q,l}^2}{2} \rho_l \left(c_{p,l} - \frac{\lambda_l}{\rho_l} \frac{\partial W_l}{\partial T} \right) \frac{\partial^3 T_l}{\partial t^3} \\ & + \omega_b c_b \tau_{q,l} \frac{\partial T_l}{\partial t} + \omega_b c_b \frac{\tau_{q,l}^2}{2} \frac{\partial^2 T_l}{\partial t^2} = k_l \left(\left(\frac{\partial^2 T_l}{\partial x^2} + \frac{\partial^2 T_l}{\partial z^2} \right) + \tau_{T_l} \frac{\partial}{\partial t} \left(\frac{\partial^2 T_l}{\partial x^2} + \frac{\partial^2 T_l}{\partial z^2} \right) + \frac{\tau_{T_l}^2}{2} \frac{\partial^2}{\partial t^2} \left(\frac{\partial^2 T_l}{\partial x^2} + \frac{\partial^2 T_l}{\partial z^2} \right) \right) \quad \text{for } l=1,2,3. \quad (19) \\ & + \omega_b c_b (T_b - T_l) + q_m + \tau_{q,l} \frac{\partial q_m}{\partial t} + \frac{\tau_{q,l}^2}{2} \frac{\partial^2 q_m}{\partial t^2} + q_{ext} + \tau_{q,l} \frac{\partial q_{ext}}{\partial t} + \frac{\tau_{q,l}^2}{2} \frac{\partial^2 q_{ext}}{\partial t^2} \end{aligned}$$

which can be written as

$$\begin{aligned}
& \rho_l c'_{p,l} \frac{\partial T_l}{\partial t} + \tau_{q,l} \rho_l c'_{p,l} \frac{\partial^2 T_l}{\partial t^2} + \frac{\tau_{q,l}^2}{2} \rho_l c'_{p,l} \frac{\partial^3 T_l}{\partial t^3} + \omega_b c_b \tau_{q,l} \frac{\partial T_l}{\partial t} + \omega_b c_b \frac{\tau_{q,l}^2}{2} \frac{\partial^2 T_l}{\partial t^2} \\
& = k_l \left(\left(\frac{\partial^2 T_l}{\partial x^2} + \frac{\partial^2 T_l}{\partial z^2} \right) + \tau_{T_l} \frac{\partial}{\partial t} \left(\frac{\partial^2 T_l}{\partial x^2} + \frac{\partial^2 T_l}{\partial z^2} \right) + \frac{\tau_{T_l}^2}{2} \frac{\partial^2}{\partial t^2} \left(\frac{\partial^2 T_l}{\partial x^2} + \frac{\partial^2 T_l}{\partial z^2} \right) \right) \quad \text{for } l=1,2,3. \quad (20) \\
& + \omega_b c_b (T_b - T_l) + q_m + \tau_{q,l} \frac{\partial q_m}{\partial t} + \frac{\tau_{q,l}^2}{2} \frac{\partial^2 q_m}{\partial t^2} + q_{ext} + \tau_{q,l} \frac{\partial q_{ext}}{\partial t} + \frac{\tau_{q,l}^2}{2} \frac{\partial^2 q_{ext}}{\partial t^2}
\end{aligned}$$

where $c'_{p,l} = \left(c_{p,l} - \frac{\lambda_l}{\rho_l} \frac{\partial W_l}{\partial T} \right)$ is the effective heat capacity

The present study considers a skin insult scenario that consists of **direct contact with a heat disk** of 1cm diameter that is maintained at a defined constant temperature for a specified time. The surface area peripheral to the disc was assumed to experience convective heat transfer with an ambient air temperature of 25°C during the burn process. After completion of the insult, the disc was removed and the entire skin surface was cooled by natural convection of the surrounding air [31, 32]. For the present scenario, the initial, boundary and interlayer conditions are stated as:

3.1.1. Initial conditions

At the initial condition, the temperature of the skin tissue is equal to the blood. Therefore,

$$t=0, T_l = T_{b,l}, \quad \frac{\partial T_l}{\partial t} = \frac{\partial^2 T_l}{\partial t^2} = 0 \quad 0 \leq x \leq L, \quad 0 \leq z \leq H, \quad (21)$$

3.1.2. The boundary conditions,

$$t > 0, \quad x=0, \quad 0 \leq z \leq H, \quad \frac{\partial T_l}{\partial x} = 0, \quad (22a)$$

$$t > 0, \quad x=L, \quad 0 \leq z \leq H, \quad \frac{\partial T_l}{\partial x} = 0, \quad (22b)$$

where $l=1, 2$

$$t > 0, \quad z=0, \quad 0 \leq x \leq L \quad \frac{\partial T_1}{\partial z} = q \quad (22c)$$

$$t > 0, \quad z=H, \quad 0 \leq x \leq L, \quad \frac{\partial T_3}{\partial z} = 0 \quad (22d)$$

3.1.3. Interlayer conditions

For the interlayers, the temperature and the heat flux in the respective layers must be equal at each point in between the layers as:

$$t > 0, \quad z = z_l, \quad 0 \leq x \leq L, \quad T_l = T_{l+1}, \quad (23a)$$

$$t > 0, \quad z = z_l, \quad 0 \leq x \leq L, \quad k_l \frac{\partial T_l}{\partial z} = k_{l+1} \frac{\partial T_{l+1}}{\partial z}, \quad (23b)$$

where $l=1, 2$

For accurate analysis, the DPL model for each layer of the skin tissue as illustrated in Fig. 2 is developed as:

3.2.1 Layer 1: Epidermis Layer

$$\begin{aligned}
& \rho_1 c'_{p,1} \frac{\partial T_1}{\partial t} + \tau_{q,1} \rho_1 c'_{p,1} \frac{\partial^2 T_1}{\partial t^2} + \frac{\tau_{q,1}^2}{2} \rho_1 c'_{p,1} \frac{\partial^3 T_1}{\partial t^3} + \omega_b c_b \tau_{q,1} \frac{\partial T_1}{\partial t} + \omega_b c_b \frac{\tau_{q,1}^2}{2} \frac{\partial^2 T_1}{\partial t^2} \\
& = k_1 \left(\left(\frac{\partial^2 T_1}{\partial x^2} + \frac{\partial^2 T_1}{\partial z^2} \right) + \tau_{T_1} \frac{\partial}{\partial t} \left(\frac{\partial^2 T_1}{\partial x^2} + \frac{\partial^2 T_1}{\partial z^2} \right) + \frac{\tau_{T_1}^2}{2} \frac{\partial^2}{\partial t^2} \left(\frac{\partial^2 T_1}{\partial x^2} + \frac{\partial^2 T_1}{\partial z^2} \right) \right) \quad (24) \\
& + \omega_b c_b (T_b - T_1) + q_m + \tau_{q,1} \frac{\partial q_m}{\partial t} + \frac{\tau_{q,1}^2}{2} \frac{\partial^2 q_m}{\partial t^2} + q_{ext} + \tau_{q,1} \frac{\partial q_{ext}}{\partial t} + \frac{\tau_{q,1}^2}{2} \frac{\partial^2 q_{ext}}{\partial t^2}
\end{aligned}$$

3.2.3 Layer 2: Dermis Layer

$$\begin{aligned}
& \rho_2 c'_{p,2} \frac{\partial T_2}{\partial t} + \tau_{q,2} \rho_2 c'_{p,2} \frac{\partial^2 T_2}{\partial t^2} + \frac{\tau_{q,2}^2}{2} \rho_2 c'_{p,2} \frac{\partial^3 T_2}{\partial t^3} + \omega_b c_b \tau_{q,2} \frac{\partial T_2}{\partial t} + \omega_b c_b \frac{\tau_{q,2}^2}{2} \frac{\partial^2 T_2}{\partial t^2} \\
& = k_2 \left(\left(\frac{\partial^2 T_2}{\partial x^2} + \frac{\partial^2 T_2}{\partial z^2} \right) + \tau_{T_2} \frac{\partial}{\partial t} \left(\frac{\partial^2 T_2}{\partial x^2} + \frac{\partial^2 T_2}{\partial z^2} \right) + \frac{\tau_{T_2}^2}{2} \frac{\partial^2}{\partial t^2} \left(\frac{\partial^2 T_2}{\partial x^2} + \frac{\partial^2 T_2}{\partial z^2} \right) \right) \\
& + \omega_b c_b (T_b - T_2) + q_m + \tau_{q,2} \frac{\partial q_m}{\partial t} + \frac{\tau_{q,2}^2}{2} \frac{\partial^2 q_m}{\partial t^2} + q_{ext} + \tau_{q,2} \frac{\partial q_{ext}}{\partial t} + \frac{\tau_{q,2}^2}{2} \frac{\partial^2 q_{ext}}{\partial t^2}
\end{aligned} \tag{25}$$

3.2.3 Layer 3: Subcutaneous Layer

$$\begin{aligned}
& \rho_3 c'_{p,3} \frac{\partial T_3}{\partial t} + \tau_{q,3} \rho_3 c'_{p,3} \frac{\partial^2 T_3}{\partial t^2} + \frac{\tau_{q,3}^2}{2} \rho_3 c'_{p,3} \frac{\partial^3 T_3}{\partial t^3} + \omega_b c_b \tau_{q,3} \frac{\partial T_3}{\partial t} + \omega_b c_b \frac{\tau_{q,3}^2}{2} \frac{\partial^2 T_3}{\partial t^2} \\
& = k_2 \left(\left(\frac{\partial^2 T_3}{\partial x^2} + \frac{\partial^2 T_3}{\partial z^2} \right) + \tau_{T_3} \frac{\partial}{\partial t} \left(\frac{\partial^2 T_3}{\partial x^2} + \frac{\partial^2 T_3}{\partial z^2} \right) + \frac{\tau_{T_3}^2}{2} \frac{\partial^2}{\partial t^2} \left(\frac{\partial^2 T_3}{\partial x^2} + \frac{\partial^2 T_3}{\partial z^2} \right) \right) \\
& + \omega_b c_b (T_b - T_3) + q_m + \tau_{q,3} \frac{\partial q_m}{\partial t} + \frac{\tau_{q,3}^2}{2} \frac{\partial^2 q_m}{\partial t^2} + q_{ext} + \tau_{q,3} \frac{\partial q_{ext}}{\partial t} + \frac{\tau_{q,3}^2}{2} \frac{\partial^2 q_{ext}}{\partial t^2}
\end{aligned} \tag{26}$$

3.3.1. Initial conditions

At the initial condition, the temperature of the skin tissue is equal to the blood and is expressed as:

$$t = 0, \quad 0 \leq x \leq L, \quad 0 \leq z \leq H, \quad T_1 = T_b, \quad \frac{\partial T_1}{\partial t} = \frac{\partial^2 T_1}{\partial t^2} = 0, \tag{27a}$$

$$t = 0, \quad 0 \leq x \leq L, \quad 0 \leq z \leq H, \quad T_2 = T_b, \quad \frac{\partial T_2}{\partial t} = \frac{\partial^2 T_2}{\partial t^2} = 0, \tag{27b}$$

$$t = 0, \quad 0 \leq x \leq L, \quad 0 \leq z \leq H, \quad T_3 = T_b, \quad \frac{\partial T_3}{\partial t} = \frac{\partial^2 T_3}{\partial t^2} = 0, \tag{27c}$$

3.3.2. The boundary conditions,

$$t > 0, \quad x = 0, \quad 0 \leq z \leq H, \quad \frac{\partial T_1}{\partial x} = 0, \tag{28a}$$

$$t > 0, \quad x = 0, \quad 0 \leq z \leq H, \quad \frac{\partial T_2}{\partial x} = 0, \tag{28b}$$

$$t > 0, \quad x = 0, \quad 0 \leq z \leq H, \quad \frac{\partial T_3}{\partial x} = 0, \tag{28c}$$

$$t > 0, \quad x = L, \quad 0 \leq z \leq H, \quad \frac{\partial T_1}{\partial x} = 0, \tag{28d}$$

$$t > 0, \quad x = L, \quad 0 \leq z \leq H, \quad \frac{\partial T_2}{\partial x} = 0, \tag{28e}$$

$$t > 0, \quad x = L, \quad 0 \leq z \leq H, \quad \frac{\partial T_3}{\partial x} = 0, \tag{28f}$$

At the surface of the skin, the heat conducted to the surface is taken as the heat lost to ambient air through convection

$$t > 0, \quad z = 0, \quad 0 \leq x \leq H \quad -k \frac{\partial T_1}{\partial z} = h_{eff} (T_a - T_1) \tag{28g}$$

where the effective convective heat transfer coefficient is given as

$$h_{eff} = h + \sigma \varepsilon (T_a + T_1) (T_a^2 + T_1^2) \tag{28h}$$

However, at the bottom of the subcutaneous layer, the local temperature is equal to the arterial temperature

$$t > 0, \quad z = H, \quad 0 \leq x \leq L, \quad T_3 = T_b \quad (28i)$$

3.3.3. Interlayer conditions

In the interlayers, the temperature and heat flux is assumed continuous across the interface. Therefore, the temperature and the heat flux in the respective layers is equal at each point amongst the layers.

$$t > 0, \quad z = z_1, \quad 0 \leq x \leq L, \quad T_1 = T_2, \quad (29a)$$

$$t > 0, \quad z = z_1, \quad 0 \leq x \leq L, \quad k_1 \frac{\partial T_1}{\partial z} = k_2 \frac{\partial T_2}{\partial z}, \quad (29b)$$

$$t > 0, \quad z = z_2, \quad 0 \leq x \leq L, \quad T_2 = T_3, \quad (29c)$$

$$t > 0, \quad z = z_2, \quad 0 \leq x \leq L, \quad k_2 \frac{\partial T_2}{\partial z} = k_3 \frac{\partial T_3}{\partial z}, \quad (29d)$$

4. Finite Element Analysis of the Thermal Model

The transient triple-layer skin thermal model in Eq. (14) is analysed using Galerkin's FEM. By applying Galerkin's method, the temperature of the cutaneous skin tissue is discretised over space as:

$$T_l(x, z, t) = \sum_{i=1}^n N_i(x, z) T_i(t) \quad (30)$$

where N_i represents the shape function, n is the number of nodes in an element and $T_i(t)$ represents the time-dependent nodal temperature. Galerkin's representation of Eq. (20) is expressed as:

$$\int_n N_i(x, z) \left[\begin{aligned} & \rho_l c'_{p,l} \frac{\partial T_l}{\partial t} + \tau_{q,l} \rho_l c'_{p,l} \frac{\partial^2 T_l}{\partial t^2} + \frac{\tau_{q,l}^2}{2} \rho_l c'_{p,l} \frac{\partial^3 T_l}{\partial t^3} + \omega_b c_b \tau_{q,l} \frac{\partial T_l}{\partial t} + \omega_b c_b \frac{\tau_{q,l}^2}{2} \frac{\partial^2 T_l}{\partial t^2} \\ & + k_l \left(\left(\frac{\partial^2 T_l}{\partial x^2} + \frac{\partial^2 T_l}{\partial z^2} \right) + \tau_{T_l} \frac{\partial}{\partial t} \left(\frac{\partial^2 T_l}{\partial x^2} + \frac{\partial^2 T_l}{\partial z^2} \right) + \frac{\tau_{T_l}^2}{2} \frac{\partial^2}{\partial t^2} \left(\frac{\partial^2 T_l}{\partial x^2} + \frac{\partial^2 T_l}{\partial z^2} \right) \right) \\ & + \omega_b c_b (T_b - T_l) + q_m + \tau_{q,l} \frac{\partial q_m}{\partial t} + \frac{\tau_{q,l}^2}{2} \frac{\partial^2 q_m}{\partial t^2} + q_{ext} + \tau_{q,l} \frac{\partial q_{ext}}{\partial t} + \frac{\tau_{q,l}^2}{2} \frac{\partial^2 q_{ext}}{\partial t^2} \end{aligned} \right] d\Omega = 0, \quad (31)$$

The above Eq. (31) can be written as:

$$\iiint_V N_i \left[\begin{aligned} & \rho_l c'_{p,l} \frac{\partial T_l}{\partial t} + \tau_{q,l} \rho_l c'_{p,l} \frac{\partial^2 T_l}{\partial t^2} + \frac{\tau_{q,l}^2}{2} \rho_l c'_{p,l} \frac{\partial^3 T_l}{\partial t^3} + \omega_b c_b \tau_{q,l} \frac{\partial T_l}{\partial t} + \omega_b c_b \frac{\tau_{q,l}^2}{2} \frac{\partial^2 T_l}{\partial t^2} \\ & + k_l \left(\left(\frac{\partial^2 T_l}{\partial x^2} + \frac{\partial^2 T_l}{\partial z^2} \right) + \tau_{T_l} \frac{\partial}{\partial t} \left(\frac{\partial^2 T_l}{\partial x^2} + \frac{\partial^2 T_l}{\partial z^2} \right) + \frac{\tau_{T_l}^2}{2} \frac{\partial^2}{\partial t^2} \left(\frac{\partial^2 T_l}{\partial x^2} + \frac{\partial^2 T_l}{\partial z^2} \right) \right) \\ & + \omega_b c_b (T_b - T_l) + q_m + \tau_{q,l} \frac{\partial q_m}{\partial t} + \frac{\tau_{q,l}^2}{2} \frac{\partial^2 q_m}{\partial t^2} + q_{ext} + \tau_{q,l} \frac{\partial q_{ext}}{\partial t} + \frac{\tau_{q,l}^2}{2} \frac{\partial^2 q_{ext}}{\partial t^2} \end{aligned} \right] dV = 0, \quad (32)$$

Applying integration by parts to Eq. (32), we have

$$\begin{aligned}
& \left[\iint_A \left\{ \left[N_i k_l \frac{\partial T_l}{\partial x} n_x \right] + \left[N_i k_l \frac{\partial T_l}{\partial z} n_z \right] + \left[N_i \left(\tau_{T_i} \frac{\partial}{\partial t} \left\{ \left[N_i k_l \frac{\partial T_l}{\partial x} n_x \right] + \left[N_i k_l \frac{\partial T_l}{\partial z} n_z \right] \right\} + \frac{\tau_{T_i}^2}{2} \frac{\partial^2}{\partial t^2} \left\{ \left[N_i k_l \frac{\partial T_l}{\partial x} n_x \right] + \left[N_i k_l \frac{\partial T_l}{\partial z} n_z \right] \right\} \right) \right\} \right] dA \\
& = \iiint_V \left\{ \left[N_i \left[\rho_l c'_{p,l} \frac{\partial T_l}{\partial t} + \tau_{q,l} \rho_l c'_{p,l} \frac{\partial^2 T_l}{\partial t^2} + \frac{\tau_{q,l}^2}{2} \rho_l c'_{p,l} \frac{\partial^3 T_l}{\partial t^3} \right] \right. \right. \\
& \quad \left. \left. + \omega_b c_b \tau_{q,l} \frac{\partial T_l}{\partial t} + \omega_b c_b \frac{\tau_{q,l}^2}{2} \frac{\partial^2 T_l}{\partial t^2} \right] \right. \\
& \quad \left. - N_i \left[\omega_b c_b (T_b - T_l) + q_m + \tau_{q,l} \frac{\partial q_m}{\partial t} + \frac{\tau_{q,l}^2}{2} \frac{\partial^2 q_m}{\partial t^2} \right] \right. \\
& \quad \left. + q_{ext} + \tau_{q,l} \frac{\partial q_{ext}}{\partial t} + \frac{\tau_{q,l}^2}{2} \frac{\partial^2 q_{ext}}{\partial t^2} \right] \Bigg\} dV \\
& + \iiint_V \left\{ \left[k_l \left[\frac{\partial T_l}{\partial x} \frac{\partial N_i}{\partial x} \right] + k_l \left[\frac{\partial T_l}{\partial z} \frac{\partial N_i}{\partial z} \right] \right. \right. \\
& \quad \left. \left. N_i \left(\tau_{T_i} \frac{\partial}{\partial t} \left\{ k_l \left[\frac{\partial T_l}{\partial x} \frac{\partial N_i}{\partial x} \right] + k_l \left[\frac{\partial T_l}{\partial z} \frac{\partial N_i}{\partial z} \right] \right\} + \frac{\tau_{T_i}^2}{2} \frac{\partial^2}{\partial t^2} \left\{ k_l \left[\frac{\partial T_l}{\partial x} \frac{\partial N_i}{\partial x} \right] + k_l \left[\frac{\partial T_l}{\partial z} \frac{\partial N_i}{\partial z} \right] \right\} \right) \right] \right\} dV \tag{35}
\end{aligned}$$

Recall that the non-Fourier's law (Dual-Phase Lag Model) in a rectangular coordinate is given by

$$q_x'' = - \left(1 + \tau_T \frac{\partial}{\partial t} + \frac{\tau_T^2}{2} \frac{\partial^2}{\partial t^2} \right) k \frac{\partial T}{\partial x}, \quad q_z'' = - \left(1 + \tau_T \frac{\partial}{\partial t} + \frac{\tau_T^2}{2} \frac{\partial^2}{\partial t^2} \right) k \frac{\partial T}{\partial z} \tag{36}$$

Substitution of Eq. (36) into Eq. (35) results in

$$\begin{aligned}
& - \left[\iint_{A^{(e)}} (N_i q_x n_x + N_i q_z n_z) dA \right] \\
& = \iiint_V \left\{ \left[N_i \left[\rho_l c'_{p,l} \frac{\partial T_l}{\partial t} + \tau_{q,l} \rho_l c'_{p,l} \frac{\partial^2 T_l}{\partial t^2} + \frac{\tau_{q,l}^2}{2} \rho_l c'_{p,l} \frac{\partial^3 T_l}{\partial t^3} \right] \right. \right. \\
& \quad \left. \left. + \omega_b c_b \tau_{q,l} \frac{\partial T_l}{\partial t} + \omega_b c_b \frac{\tau_{q,l}^2}{2} \frac{\partial^2 T_l}{\partial t^2} \right] \right. \\
& \quad \left. - N_i \left[\omega_b c_b (T_b - T_l) + q_m + \tau_{q,l} \frac{\partial q_m}{\partial t} + \frac{\tau_{q,l}^2}{2} \frac{\partial^2 q_m}{\partial t^2} \right] \right. \\
& \quad \left. + q_{ext} + \tau_{q,l} \frac{\partial q_{ext}}{\partial t} + \frac{\tau_{q,l}^2}{2} \frac{\partial^2 q_{ext}}{\partial t^2} \right] \Bigg\} dV \\
& + \iiint_V \left\{ \left[k_l \left[\frac{\partial T_l}{\partial x} \frac{\partial N_i}{\partial x} \right] + k_l \left[\frac{\partial T_l}{\partial z} \frac{\partial N_i}{\partial z} \right] \right. \right. \\
& \quad \left. \left. N_i \left(\tau_{T_i} \frac{\partial}{\partial t} \left\{ k_l \left[\frac{\partial T_l}{\partial x} \frac{\partial N_i}{\partial x} \right] + k_l \left[\frac{\partial T_l}{\partial z} \frac{\partial N_i}{\partial z} \right] \right\} + \frac{\tau_{T_i}^2}{2} \frac{\partial^2}{\partial t^2} \left\{ k_l \left[\frac{\partial T_l}{\partial x} \frac{\partial N_i}{\partial x} \right] + k_l \left[\frac{\partial T_l}{\partial z} \frac{\partial N_i}{\partial z} \right] \right\} \right) \right] \right\} dV \tag{37}
\end{aligned}$$

Eq. (37) can be written as

results in a large number of algebraic equations in matrix form termed global matrix. The global matrix governs the whole domain of the problem under investigation. The boundary conditions of the problem are imposed on the assembled equations in the global matrix. The resulting system of equations is solved numerically until the desired accuracy or convergence criterion is achieved. The convergence criterion of the numerical solution along with the error estimation has been set to

$$\sum_w^N |T^w - T^{w-1}| \leq 10^{-6} \quad (43)$$

where T is the general dependent variable and w is the number of iteration

It is worth noting that the boundary conditions and the temperature-dependent parameters are incorporated in the computer program used to solve the system of algebraic equations.

5. Thermal Damage Model and Classification of Degree of Burns

Skin thermal damage starts when the basal epidermis temperature reaches 44°C . To evaluate the degree and rate of thermal damage to the skin tissues, the following rate model is developed.

$$\frac{d\Omega_l}{dt} = \begin{cases} 0 & T < 44^\circ\text{C} \\ Ae^{-\frac{E_a}{RT_l(x,z,t)}} & T \geq 44^\circ\text{C} \end{cases} \quad (44)$$

where Ω_l , t , A , E_a , R and T_l represents the thermal damage in tissue, time, frequency factor, the activation energy for skin, universal gas constant and temperature of layer l respectively. Hence, by integrating the Eq. (32), we have

$$\Omega_l = \begin{cases} 0 & T < 44^\circ\text{C} \\ \int_0^t Ae^{-\frac{E_a}{RT_l(x,z,t)}} dt & T \geq 44^\circ\text{C} \end{cases} \quad (45)$$

Eq. (32) predicts the thermal damage Ω , which is a key prediction parameter to determine the degree of burn for clinical decision and treatment of damaged skin [38]. Moreover, the value of Ω determines the degree of the burn by the burn depth as presented in Table 1.

Table 1. Burn degree and its associated biological features

Burn	Ω	Biological features
First-degree (Superficial or epidermal burns)	0.53	affects epidermis with vasodilatation of the sub-capillary vessels, redness of affected area with no permanent scars or discolouration, mild pain and healing is rapid
Second-degree (Partial-thickness burns)	1.0	Both epidermis and dermis are slightly affected. Burn can be superficial or deep. Superficial burn results in moist blisters, whilst deep burn affects the capillaries or blood vessels causing tissue oedema and blisters on the skin
Third-degree (Full Thickness)	10000	Both epidermis and dermis are thermally damaged, causing blood flow to stop. The cells around the burn region start to die leading to leathery skin. Recovery from burn degree requires special treatment

It is worth noting that the developed skin burns model is used to determine the required time to generate the different degrees of burns on the human body based on the understanding of the classification in Table 1.

6. Results and Discussion

The above-developed solutions are simulated and the effects of various thermal and flow parameters on temperature for the assessment of burn injury are investigated. The effects of thermal conductivity of the triple layer of the skin for prediction of burn injury baseline are presented in Figs. 2, 3 and 4. In Fig. 2, as the thermal conductivity of the epidermis increases by factor of 2, the injury baseline shifts towards the left-hand side (LHS) of the base value (0.210W/mK). This is because, as the thermal conductivity of the epidermis increases under continuous temperature exposure, the thermal resistance reduces resulting in increased heat penetration of the tissue. Under this condition, the time required to reach a second-degree burn injury situation becomes minimal.

This shows that the higher the thermal conductivity of the skin tissue, the greater the degree of burn.

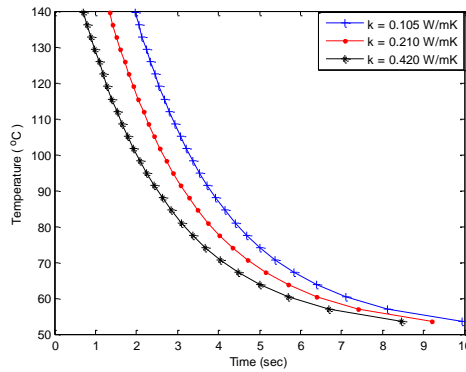


Fig. 2. Effects of thermal conductivity of epidermis on burn injury baseline

Moreover, the opposite trend is observed as the thermal conductivity decreases by factor of 2, which results in the injury baseline shifting towards the right-hand side (RHS) of the base value (0.210W/mK). This is because as thermal conductivity reduces, the thermal resistance increases resulting in reduced heat penetration of the tissue. Consequently, under such burns condition, more time would be required to reach a second-degree burn injury.

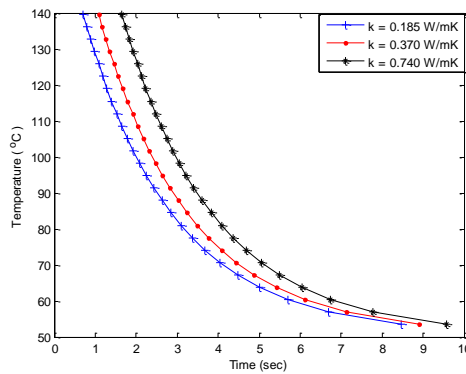


Fig. 3. Effects of dermis thermal conductivity on burn injury baseline

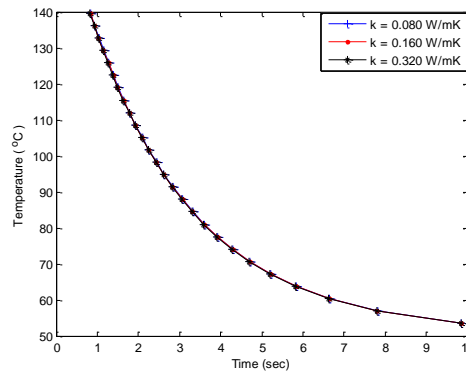


Fig. 4. Effects of subcutaneous layer thermal conductivity on burn injury baseline

Fig. 3 shows that as the thermal conductivity of the dermis increases by factor of 2, the injury baseline shifts towards the RHS of the base value, i.e., 0.370W/mK. This phenomenon occurs, as an increase in the dermis thermal conductivity causes heat at the epidermis-dermis interface to be readily transferred to the deeper tissue and consequently resulting in prolonged time required to reach the injury baseline. However, an opposite trend is observed when the thermal conductivity of the dermis is decreased by factor of 2, resulting in the injury baseline shifting towards the LHS of the base value (0.370W/mK). Moreover, the above finding implies that the thermal conductivity of the dermis reduces as the temperature of exposure heat decreases. **Fig. 4 illustrates the effect of the subcutaneous layer thermal conductivity on burn injury baseline. It is worth noting that the three curves lie on top of each other.** This shows that the thermal conductivity of the subcutaneous layer exhibits no significant effect on the prediction of the injury baseline.

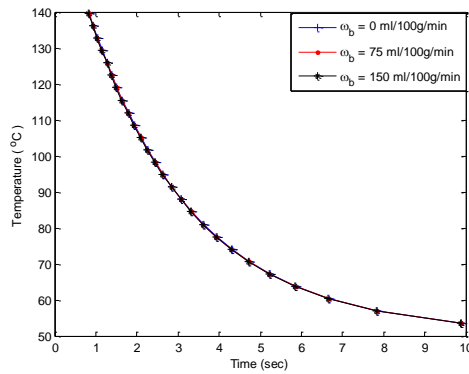


Fig. 5. Effects of blood perfusion rate on burn injury baseline

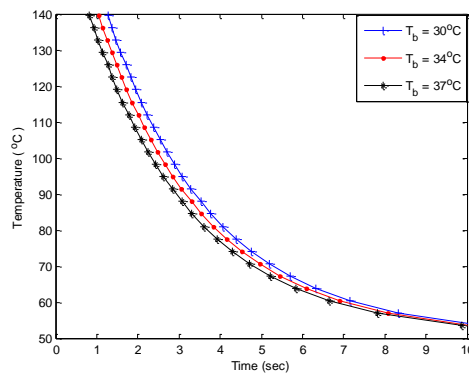


Fig. 6. Effects of initial skin tissue temperature on burn injury baseline

Fig. 5 illustrates the effect of blood perfusion rate on the prediction baseline. Under constant volumetric capacity of the blood, the effects of no perfusion (0ml/100g/min), half of the maximum dilatation (75ml/100g/min) and maximum blood flow (150ml/100g/min) of the skin vessels. From Fig. 5, the blood perfusion rate exhibits negligible effects on the dermis and invariably does not affect the burn injury prediction in the dermis layer. The effects of initial skin tissue temperature on the burn injury baseline prediction are presented in Fig. 6. From Fig. 6, the initial skin tissue temperature exhibits significant effects on skin exposed to burn injury. This is because the warmth of the skin tissue increases as the temperature experienced throughout the heating and cooling periods increases resulting in an increased degree of burn injury.

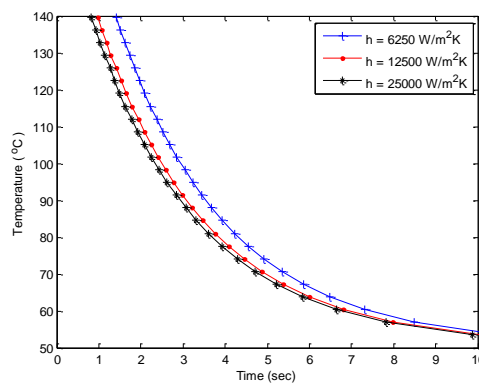


Fig. 7. Effects of convective heat transfer coefficient on burn injury baseline

The effect of convective heat transfer coefficient for the prediction of burn injury baseline is illustrated in Fig. 7. In Fig. 7, it is shown that the heat transfer coefficient exhibits significant effects on the burn injury baseline for minimal exposure time. However, the effect of the convective heat transfer coefficient becomes negligible, with prolonged exposure time. This is because, under prolonged exposure of the skin layers to burn, the burn injury is dominated by conductive heat transfer in the tissue rather than the convective heat transfer at the surface of the skin. Moreover, as the convective heat transfer coefficient increases by a factor of 2, the injury baseline shifts towards the LHS of the base value (1250W/m²K).

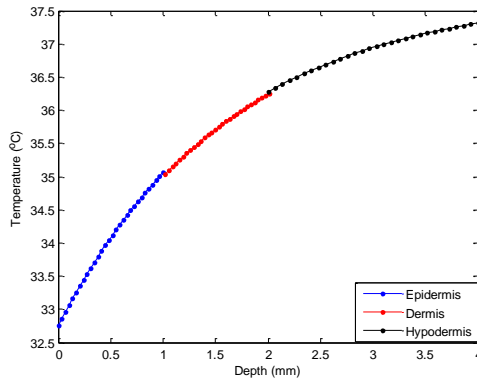


Fig. 8. Initial tissue temperature profiles for three-layer skin tissue

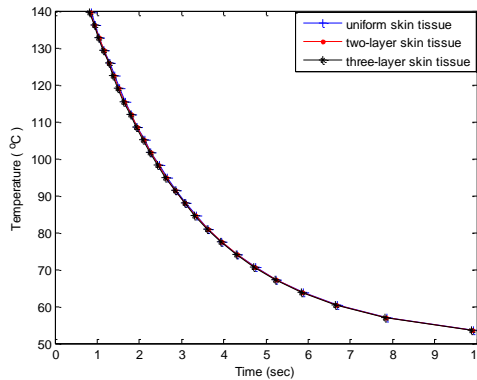


Fig. 9. Injury baseline with uniform tissue temperature (34°C) and initial temperature profile for two-layer and three-layer slab

Under such condition, minimal time is required to reach the second-degree injury baseline. However, when the convective heat transfer coefficient is decreased by a factor of 2, the injury baseline shifts towards the RHS of the base value (1250W/m²K), which shows that as the convective heat transfer coefficient decreases, more time is needed for the skin burn to reach a second-degree burn injury. Fig. 8 shows the initial tissue temperature profiles for the three-layer skin tissue whilst the injury baseline using a uniform tissue temperature of 34°C and the initial temperature profile for two and three-layer slabs is presented in Fig. 9. Figs 8 and 9 shows that the selection of initial temperature 34°C for all the three layers is highly reasonable. It is worth noting that uniform initial temperature can be applied for all three layers for a more accurate analysis of the cutaneous tissue burn injury. Moreover, the skin injury layer baseline range of combinations of different values of thermal properties is presented in Fig. 10. Fig. 10 considers the effect of a worst-case combination of parameters, where the upper baseline represents a combination of low thermal properties of skin components, low heat transfer coefficient and low initial tissue temperature. The lower baseline represents a combination of high values of these parameters.

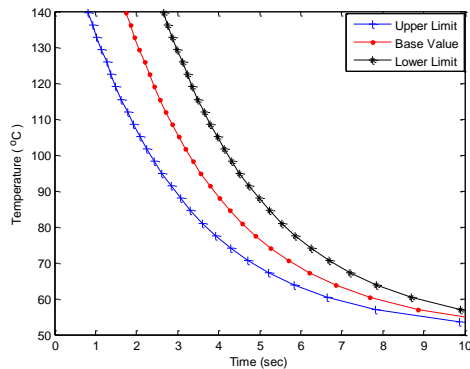


Fig. 10. Skin injury layer baselines for varying thermal properties

6.1. Effects of Relaxation time and Thermalisation time

The effects of relaxation time and thermalisation time on the skin temperature during the cooling process is presented in Fig. 11. The simulation shows that the peak temperature predicted by the classical bioheat equation is higher than the DPL during the heating process. However, the temperatures from all considered cases converge during the cooling process. This is because the finite speed of wave propagation and the peak temperature predicted by the DPL occurs with time lags. The time lag causes longer thermal dissipation, i.e., cooling by the heat conduction of tissue and by the blood perfusion period of peak temperature. The predicted higher temperature by the classical bioheat model than the DPL model implies that the accumulation of the thermal damage is overestimated since the level of the accumulative thermal damage depends primarily on the peak temperature. Moreover, as seen in Fig. 11, the relaxation time and thermalisation time enhances heat diffusion and reduces the thermal damage in the skin tissues. This effect is noticeable as the heat transfer process approaches the peak temperature during heating. However, the curves are close and almost similar values are predicted during cooling for the relaxation time and thermalisation time considered.

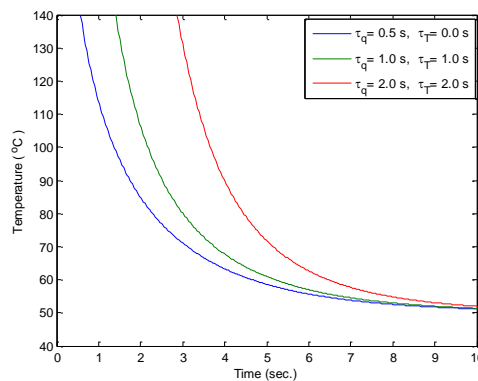
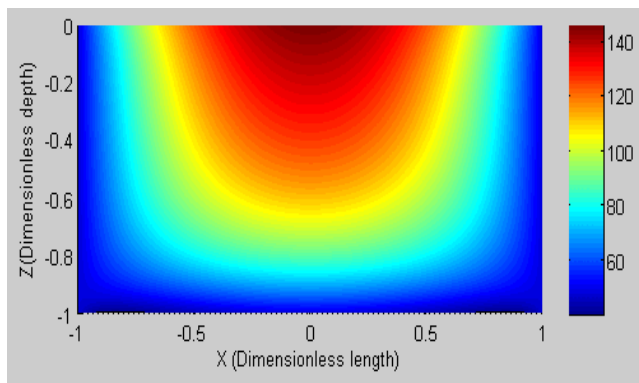
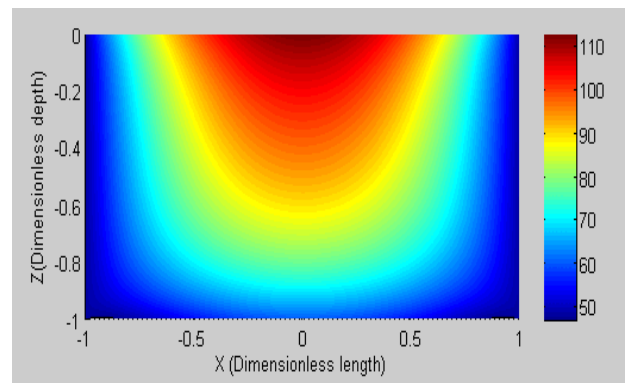


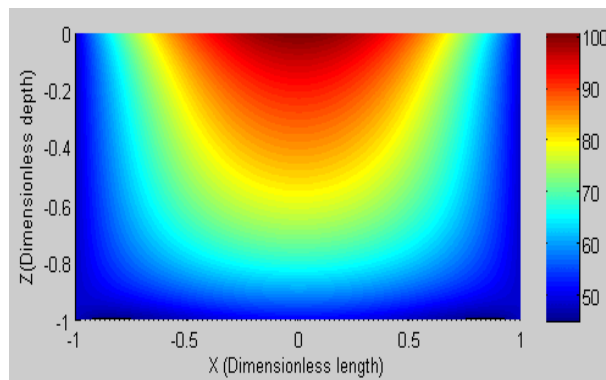
Fig. 11. Effects of relaxation time and thermalisation time on the skin temperature



a. Maximum temperature distribution in the skin tissue before cooling



b. Temperature distribution in the skin tissue after 4sec of cooling



c. Maximum temperature distribution in the skin tissue after 7sec of cooling

Fig. 12. Temperature distribution of the skin tissue before and after cooling

The temperature distribution in the skin tissue at depth 0.006m and length 0.024m for a period of 8sec are presented in Fig. 12. Fig. 12 shows the dimensionless length and depth of the tissue, where the negative values in the dimensionless depth indicate depth zero i.e., below the skin surface. The dimensional length ranges from -1 to +1 to depict symmetry as stated in the boundary conditions. The dimensional length ranges from -1 to +1 to depict symmetry as stated in the boundary conditions. Further, the results of the present study are compared with the different established works in the literature including Henriques [39], Fugitt et al. [40], Stoll and Greene [41], Takata [42] and Wu [43] as presented in Figs. 13-18. Fig. 13 demonstrates the comparison of the various results for the effects of surface temperature on burn injury. Also, Figs. 14 - 16 demonstrates the required time to reach the first, second and third-degree burn injuries when the skin tissue temperature is maintained at 50°C, 70°C, and 90°C respectively. The effects of tissue depth and surface temperature on the degree of burn and burn injury are illustrated in Figs. 17 and 18. It is shown that the thermal damage value or the value of the burn injury is minimal for low tissue temperature but increases rapidly with temperature above 50°C.

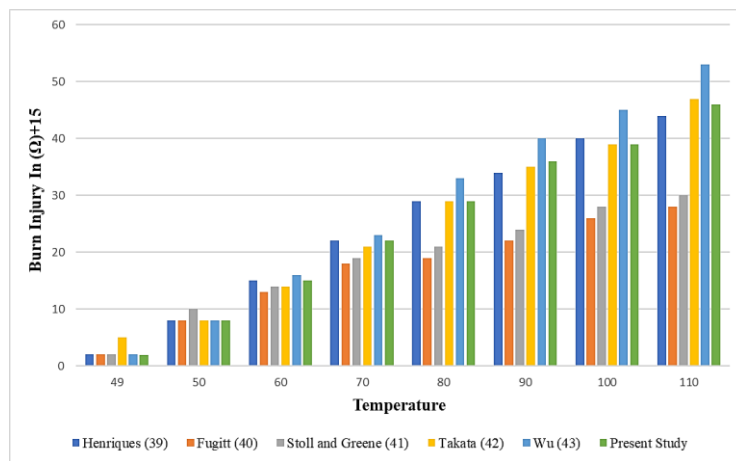


Fig. 13. Comparison of present work with existing studies on the effect of surface temperature on burn injury

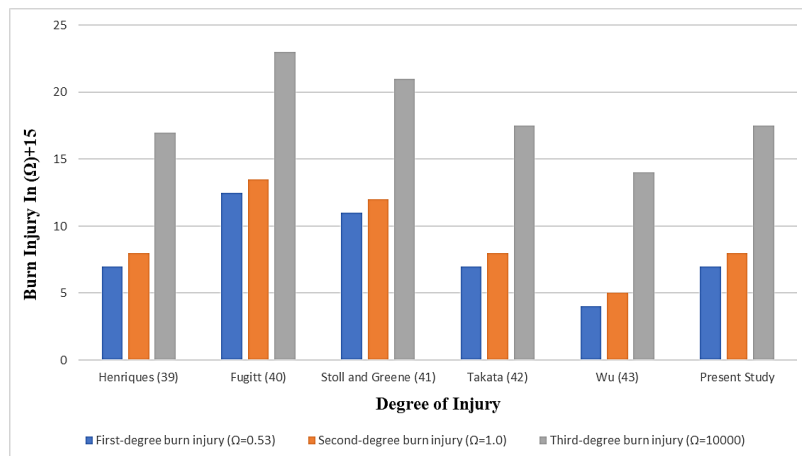


Fig. 14. Comparison of present work with existing studies on degree of burn and burn injury time (log) at fixed surface temperature of 50°C

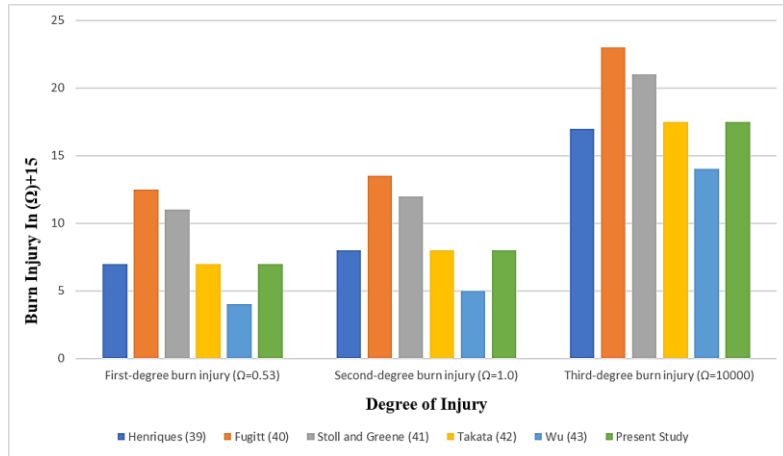


Fig. 15. Comparison of present work with existing studies on degree of burn and burn injury time (log) at fixed surface temperature of 70°C

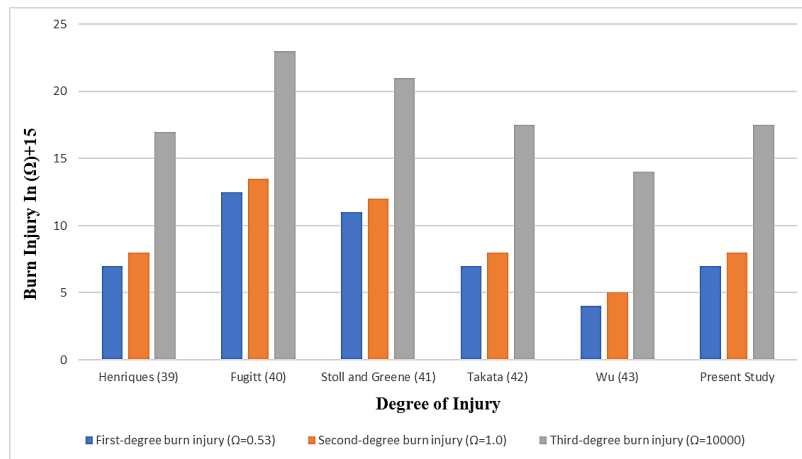


Fig. 16. Comparison of present work with existing studies on degree of burn and burn injury time (log) at fixed surface temperature of 90°C

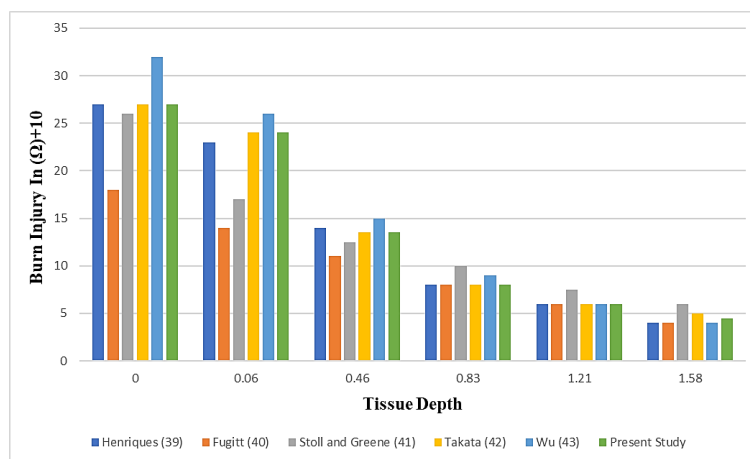


Fig. 17. Comparison of present work with existing studies on the degree of burn injury for various tissue depth at 80°C for 5s

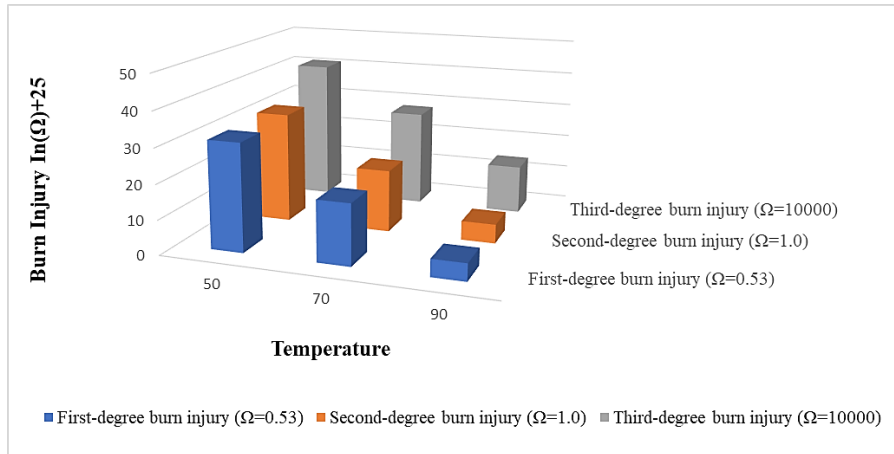


Fig. 18. Comparison of results for the effects of temperature on the degree of burn and its associated level of injury

Figs. 13-18 show that the present study quantitatively agrees with previous studies for low-level damage at temperatures below 50°C. However, there is significant variation among the skin burn damage models results for high exposure temperatures. In fact, for temperature above 50°C, only Henriques [39] and Takata [42] corresponds reasonably for all temperatures evaluated and in agreement with the results of the present study. Fig. 19 presents the validation of the present study with the experimental work of Takata [42]. From the comparison, the present study shows significant agreements with the experimental work of Takata [42], which demonstrates the reliability of the obtained results of the study.

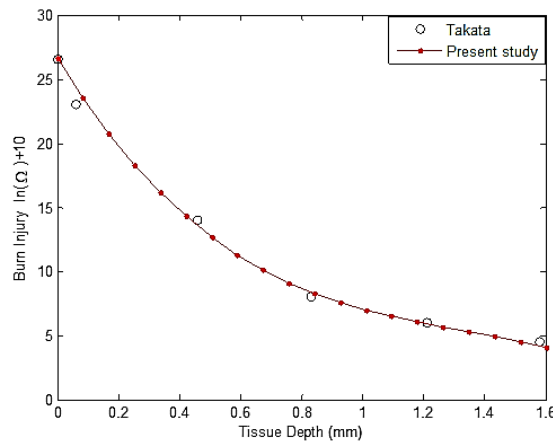


Fig. 19. Comparison of the present study on burn injury with established experimental results

7. Conclusion

In the present work, Galerkin's finite element method is used to analyse the DPL bioheat model of the human skin. The effects of skin tissue properties, initial temperature, blood perfusion rate, relaxation and thermalisation time and heat transfer parameters for the thermal response and exposure time of triple-layer cutaneous tissue is carried out. The following concluding remarks are drawn from the detailed study:

- An increase in the thermal conductivity of the epidermis decreases the thermal resistance, which readily causes increased heat penetration of the tissue, which implies that the higher the thermal conductivity of the tissue, the lower the degree of burn injury
- The study shows that an increase in dermis thermal conductivity results in a prolonged time to reach the injury threshold and the blood perfusion rate exhibits no net effect on the prediction of burn injury in the dermis layer. However, the initial skin tissue temperature exhibit significant effects on burn injury exposure
- The relaxation and thermalisation time play fundamental roles in the analysis of burn injury. The relaxation time and thermalisation time enhances the heat diffusion and reduces the thermal damage in the skin tissues

- The heat transfer coefficient plays significant effects on burn injury for small exposure time. The effect of the convective heat transfer coefficient becomes minimal for prolonged exposure time.
- For accurate analysis of the skin tissue burn injury, it is convenient to use uniform initial temperature for the triple-layer cutaneous layers
- The most dominating factors in the burn injury follow the order: relaxation time and thermalisation time, initial tissue temperature followed by the epidermis layer thermal conductivity, dermis layer thermal conductivity and convective heat transfer coefficient

The present work would help in the quantification of skin burn, and for clinicians and biomedical engineers to experiment, design, characterise and optimise strategies for delivering thermal therapies.

References

- [1] J. M. Duke, S. M. Randall, M. W. Fear, J. H. Boyd, S. Rea, and F. M. Wood, "Burn induced nervous system morbidity among burn and non-burn trauma patients compared with non-injured people," *Burns*, vol. 45, no. 5, pp. 1041-1050, 2019/08/01/ 2019, doi: <https://doi.org/10.1016/j.burns.2018.06.006>.
- [2] H. H. Pennes, "Analysis of Tissue and Arterial Blood Temperatures in the Resting Human Forearm," *Journal of Applied Physiology*, vol. 1, no. 2, pp. 93-122, 1948, doi: 10.1152/jappl.1948.1.2.93.
- [3] J. Dutta and B. Kundu, "Two-dimensional closed-form model for temperature in living tissues for hyperthermia treatments," *Journal of Thermal Biology*, vol. 71, pp. 41-51, 2018/01/01/ 2018, doi: <https://doi.org/10.1016/j.jtherbio.2017.10.012>.
- [4] C. Cattaneo, J. Kampé de Fériet, and s. Académie des, *Sur une forme de l'équation de la chaleur éliminant le paradoxe d'une propagation instantanée*. [Paris]: [Gauthier-Villars] (in French), 1958.
- [5] P. Vernotte, "Les paradoxes de la theorie continue de l'equation de la chaleur," *Compt. Rendu*, vol. 246, pp. 3154-3155, 1958 1958. [Online]. Available: <https://ci.nii.ac.jp/naid/10018606050/en/>.
- [6] B. Kundu and D. Dewanjee, "A new method for non-Fourier thermal response in a single layer skin tissue," *Case Studies in Thermal Engineering*, vol. 5, pp. 79-88, 2015/03/01/ 2015, doi: <https://doi.org/10.1016/j.csite.2015.02.001>.
- [7] Z.-S. Deng and J. Liu, "Non-Fourier Heat Conduction Effect on Prediction of Temperature Transients and Thermal Stress in Skin Cryopreservation," *Journal of Thermal Stresses*, vol. 26, pp. 779 - 798, 2003.
- [8] S.-M. Lin, "Analytical Solutions of Bio-Heat Conduction on Skin in Fourier and Non-Fourier Models," *Journal of Mechanics in Medicine and Biology*, vol. 13, no. 04, p. 1350063, 2013, doi: 10.1142/s0219519413500632.
- [9] L. Wang, "Generalized Fourier law," *International Journal of Heat and Mass Transfer*, vol. 37, no. 17, pp. 2627-2634, 1994/11/01/ 1994, doi: [https://doi.org/10.1016/0017-9310\(94\)90380-8](https://doi.org/10.1016/0017-9310(94)90380-8).
- [10] D. Y. Tzou, "A Unified Field Approach for Heat Conduction From Macro- to Micro-Scales," *Journal of Heat Transfer*, vol. 117, no. 1, pp. 8-16, 1995, doi: 10.1115/1.2822329.
- [11] D. Y. Tzou, *Macro- to Microscale Heat Transfer: The Lagging Behavior*, 2nd ed. Chichester, West Sussex, PO19 8SQ, United Kingdom: John Wiley & Sons, 2015.
- [12] D. Y. Tzou, M. N. Ozisik, and R. J. Chiffelle, "The Lattice Temperature in the Microscopic Two-Step Model," *Journal of Heat Transfer*, vol. 116, no. 4, pp. 1034-1038, 1994, doi: 10.1115/1.2911439.
- [13] M. N. Ozisik and D. Y. Tzou, "On the Wave Theory in Heat Conduction," *Journal of Heat Transfer*, vol. 116, no. 3, pp. 526-535, 1994, doi: 10.1115/1.2910903.
- [14] K. J. Chua, S. K. Chou, and J. C. Ho, "An analytical study on the thermal effects of cryosurgery on selective cell destruction," (in eng), *J Biomech*, vol. 40, no. 1, pp. 100-116, 2007, doi: 10.1016/j.jbiomech.2005.11.005.
- [15] S. Singh and S. Kumar, "A Study on the Effect of Metabolic Heat Generation on Biological Tissue Freezing," *The Scientific World Journal*, vol. 2013, p. 398386, 2013/11/05 2013, doi: 10.1155/2013/398386.
- [16] A. Moradi and H. Ahmadikia, "Numerical study of the solidification process in biological tissue with blood flow and metabolism effects by the dual phase lag model," *Proceedings of the Institution of Mechanical Engineers, Part H: Journal of Engineering in Medicine*, vol. 226, no. 5, pp. 406-416, 2012.
- [17] K.-C. Liu, Y.-N. Wang, and Y.-S. Chen, "Investigation on the bio-heat transfer with the dual-phase-lag effect," *International Journal of Thermal Sciences*, vol. 58, pp. 29-35, 2012/08/01/ 2012, doi: <https://doi.org/10.1016/j.ijthermalsci.2012.02.026>.
- [18] N. Afrin, J. Zhou, Y. Zhang, D. Y. Tzou, and J. K. Chen, "Numerical Simulation of Thermal Damage to Living Biological Tissues Induced by Laser Irradiation Based on a Generalized Dual Phase Lag Model," *Numerical Heat Transfer, Part A: Applications*, vol. 61, no. 7, pp. 483-501, 2012/04/01 2012, doi: 10.1080/10407782.2012.667648.

- [19] J. Zhou, Y. Zhang, and J. K. Chen, "An axisymmetric dual-phase-lag bioheat model for laser heating of living tissues," *International Journal of Thermal Sciences*, vol. 48, no. 8, pp. 1477-1485, 2009/08/01/ 2009, doi: <https://doi.org/10.1016/j.ijthermalsci.2008.12.012>.
- [20] K.-C. Liu and H.-T. Chen, "Investigation for the dual phase lag behavior of bio-heat transfer," *International Journal of Thermal Sciences*, vol. 49, no. 7, pp. 1138-1146, 2010/07/01/ 2010, doi: <https://doi.org/10.1016/j.ijthermalsci.2010.02.007>.
- [21] E. Majchrzak and Ł. Turchan, "Numerical modeling of a hyperthermia therapy using dual-phase-lag model of bioheat transfer " in *CMM-2011 - Computer Methods in Mechanics*, Warsaw, Poland 9–12 May 2011 2011.
- [22] H. Ahmadikia, A. Moradi, R. Fazlali, and A. B. Parsa, "Analytical solution of non-Fourier and Fourier bioheat transfer analysis during laser irradiation of skin tissue," *Journal of Mechanical Science and Technology*, vol. 26, no. 6, pp. 1937-1947, 2012/06/01 2012, doi: 10.1007/s12206-012-0404-9.
- [23] J. Zhou, J. K. Chen, and Y. Zhang, "Dual-phase lag effects on thermal damage to biological tissues caused by laser irradiation," (in eng), *Comput Biol Med*, vol. 39, no. 3, pp. 286-93, Mar 2009, doi: 10.1016/j.combiomed.2009.01.002.
- [24] K.-C. Liu, P.-J. Cheng, and Y.-N. Wang, "Analysis of Non-Fourier Thermal Behaviour for Multi-Layer Skin Model," *Thermal Science*, vol. 15, pp. 61-67, 2011.
- [25] J. Ma, X. Yang, Y. Sun, and J. Yang, "Thermal damage in three-dimensional vivo bio-tissues induced by moving heat sources in laser therapy," *Scientific Reports*, vol. 9, no. 1, p. 10987, 2019/07/29 2019, doi: 10.1038/s41598-019-47435-7.
- [26] M. Mohajer, M. B. Ayani, and H. B. Tabrizi, "Numerical study of non-Fourier heat conduction in a biolayer spherical living tissue during hyperthermia," *Journal of Thermal Biology*, vol. 62, pp. 181-188, 2016/12/01/ 2016, doi: <https://doi.org/10.1016/j.jtherbio.2016.06.019>.
- [27] G. Oguntala, V. Indramohan, S. Jeffery, and R. Abd-Alhameed, "Triple-layer Tissue Prediction for Cutaneous Skin Burn Injury: Analytical Solution and Parametric Analysis," *International Journal of Heat and Mass Transfer*, vol. 173, p. 120907, 2021. [Online]. Available: <https://www.sciencedirect.com/science/article/pii/S0017931021000107>.
- [28] D. A. Torvi and J. D. Dale, "A Finite Element Model of Skin Subjected to a Flash Fire," *Journal of Biomechanical Engineering*, vol. 116, no. 3, pp. 250-255, 1994, doi: 10.1115/1.2895727.
- [29] J. Lang, B. Erdmann, and M. Seebass, "Impact of nonlinear heat transfer on temperature control in regional hyperthermia," *IEEE Transactions on Biomedical Engineering*, vol. 46, no. 9, pp. 1129-1138, 1999, doi: 10.1109/10.784145.
- [30] E. Y. K. Ng and L. T. Chua, "Comparison of one- and two-dimensional programmes for predicting the state of skin burns," *Burns*, vol. 28, no. 1, pp. 27-34, 2002/02/01/ 2002, doi: [https://doi.org/10.1016/S0305-4179\(01\)00066-3](https://doi.org/10.1016/S0305-4179(01)00066-3).
- [31] X. J. Zhao and H. Wang, "Numerical Simulation of Transient Thermal Effects in Skin Tissue," in *2011 5th International Conference on Bioinformatics and Biomedical Engineering*, 10-12 May 2011 2011, pp. 1-4, doi: 10.1109/icbbe.2011.5780375.
- [32] E. Y.-K. Ng and L. T. Chua, "Prediction of skin burn injury. Part 1: Numerical modelling," *Proceedings of the Institution of Mechanical Engineers, Part H: Journal of Engineering in Medicine*, vol. 216, no. 3, pp. 157-170, 2002, doi: 10.1243/0954411021536379.
- [33] V. V. Tuchin, "Tissue Optics and Photonics: Light-Tissue Interaction II," *Journal of Biomedical Photonics & Engineering*, vol. 2, no. 3, 2016, doi: 10.18287/JBPE16.02.030201.
- [34] M. A. Ansari, M. Erfanzadeh, and E. Mohajerani, "Mechanisms of Laser-Tissue Interaction: II. Tissue Thermal Properties," (in eng), *J Lasers Med Sci*, vol. 4, no. 3, pp. 99-106, Summer 2013. [Online]. Available: <https://www.ncbi.nlm.nih.gov/pmc/articles/PMC4295363/>.
- [35] H. Ai, S. Wu, H. Gao, L. Zhao, C. Yang, and Y. Zeng, "Temperature distribution analysis of tissue water vaporization during microwave ablation: Experiments and simulations," *International Journal of Hyperthermia*, vol. 28, no. 7, pp. 674-685, 2012/11/01 2012, doi: 10.3109/02656736.2012.710769.
- [36] J. P. Abraham and E. M. Sparrow, "A thermal-ablation bioheat model including liquid-to-vapor phase change, pressure- and necrosis-dependent perfusion, and moisture-dependent properties," *International Journal of Heat and Mass Transfer*, vol. 50, no. 13, pp. 2537-2544, 2007/07/01/ 2007, doi: <https://doi.org/10.1016/j.ijheatmasstransfer.2006.11.045>.
- [37] D. Yang, M. C. Converse, D. M. Mahvi, and J. G. Webster, "Expanding the Bioheat Equation to Include Tissue Internal Water Evaporation During Heating," *IEEE Transactions on Biomedical Engineering*, vol. 54, no. 8, pp. 1382-1388, 2007, doi: 10.1109/TBME.2007.890740.
- [38] D. P. Orgill, M. G. Solari, M. S. Barlow, and N. E. O'Connor, "A finite-element model predicts thermal damage in cutaneous contact burns," (in eng), *J Burn Care Rehabil*, vol. 19, no. 3, pp. 203-9, May-Jun 1998, doi: 10.1097/00004630-199805000-00003.

- [39] F. C. Henriques, Jr., "Studies of thermal injury; the predictability and the significance of thermally induced rate processes leading to irreversible epidermal injury," (in eng), *Arch Pathol (Chic)*, vol. 43, no. 5, pp. 489-502, May 1947.
- [40] C. E. Fugitt, "A rate process of thermal injury," 1955.
- [41] A. M. Stoll and L. C. Greene, "Relationship between pain and tissue damage due to thermal radiation," *Journal of Applied Physiology*, vol. 14, no. 3, pp. 373-382, 1959, doi: 10.1152/jappl.1959.14.3.373.
- [42] A. Takata, "Development of Criterion for Skin Burns," *Aerosp. Med*, vol. 45, pp. 634-637, 1974.
- [43] Y. C. Wu, "A Modified Criterion for Predicting Thermal Injury," National Bureau of Standards, USA, 1980.